

# A Practical Tool for Predicting the Minimum Ignition Energy of Organic Dusts

Sabrina Copelli, Martina S. Scotton, Marco Barozzi, Marco Derudi, and Renato Rota\*



Cite This: *Ind. Eng. Chem. Res.* 2021, 60, 10807–10813



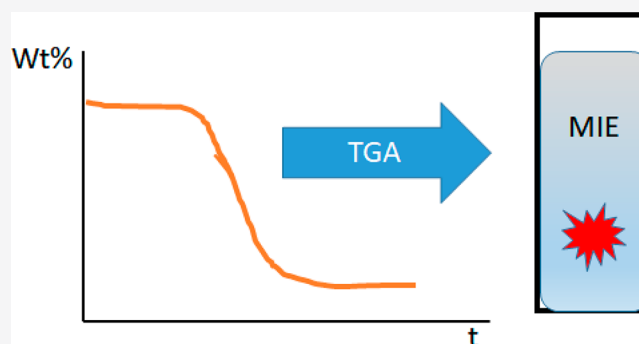
Read Online

ACCESS |

Metrics & More

Article Recommendations

**ABSTRACT:** In the last decades, protection and prevention in the workplace has assumed great relevance. In this context, organic dust explosions represent one of the major risks. Within this frame, the minimum ignition energy (MIE) of a dust occupies a fundamental role for the assessment of the explosibility hazard. At present, the measurement of the MIE is performed using the standard Hartmann apparatus. This approach involves some practical limitations, mainly related to the testing times and costs. This work is focused on developing both a mathematical model capable of describing the main phenomena leading to the ignition of an organic dust inside a Hartmann tube and a simpler procedure for the estimation of the MIE. Such an approach relies on the use of accessible physicochemical properties and simple thermogravimetric analysis (TGA) experiments, coupled with a particle size analysis capable of providing a mean characteristic diameter of the dust. The proposed procedure has been validated by comparison with literature experimental data of minimum ignition energy of several organic dusts, showing a fair agreement among experimental results and model predictions.



## 1. INTRODUCTION

Industrial safety has been always a subject of great concern, especially in recent years, because of the relatively high number of industrial accidents and negative associated consequences. In 2020, the number of major accidents that occurred in industrial facilities increased globally, especially because of the post-lockdown refurbishment of plants.<sup>1</sup> According to a report published by the Industrial Global Union<sup>2</sup> in India, there was an average of one accident and one death per alternate day only in the month of May 2020 and, among the months of January and August 2020, there were at least 25 serious industrial accidents, which caused over than 120 deaths. There were also reports of similar accidents in the industrial facilities restarted up in other parts of Asia, as well as Italy, Turkey, and the United States. Also, according to CCPS,<sup>3</sup> it is well-known that process safety accidents occur five times more frequently during start-up and shut-down operations than during normal activities. Moreover, industrial accidents are not only related to the re-startup of plants after a prolonged stop, but they can be also connected to normal operations or storage of potentially dangerous materials in warehouses. This is what happened in Beirut on August 2020, where a large amount of ammonium nitrate stored in a port warehouse exploded, causing at least 203 deaths and 6500 injuries.<sup>4</sup> With regard to dust explosions, in 2019, 87% of the global fatalities recorded occurred because of dust explosions and, of this percentage, up to 65% were due to organic dusts such as wood and food products;<sup>5</sup>

furthermore, in the first semester of 2020, 26 dust explosions occurred worldwide, and 80% of them were caused by organic dusts.<sup>6</sup> Such data simply confirm the importance of increasing the safety of plants managing explosive dusts through the implementation of risk assessment procedures using either traditional methods, such as HazOp, FTA, FMEA, or innovative ones, such as ROA-ISD,<sup>7,8</sup> which is specifically tailored for organic dust explosions.

Regardless of the method used for risk assessment, the knowledge of the explosive characteristics of the powder (usually summarized in a few parameters, such as the deflagration index ( $K_{St}$ ), the lower explosive limit (LEL), the minimum ignition energy (MIE), etc.) is of paramount importance to provide an extent of the probability of occurrence of a dust explosion.<sup>9</sup> Such explosive parameters for a given dust are usually estimated by experimental tests, therefore requiring high costs and long times. Moreover, it is quite cumbersome to test all the different particle size distributions that can be present in a real plant where several

**Special Issue:** Giuseppe Storti Festschrift

**Received:** January 21, 2021

**Revised:** March 21, 2021

**Accepted:** March 26, 2021

**Published:** May 27, 2021



unit operations (e.g., milling, granulation, etc.) are usually involved. This is the reason because some predictive mathematical models have been recently proposed in the literature for estimating some of these explosive parameters.<sup>10–12</sup>

Concerning the estimation of the MIE, some predictive methods based on both group contribution models<sup>13</sup> and hybridization of gravitational search algorithm (GSA) with support vector regression (SVR), using relatively few descriptors (which include the number of carbon and hydrogen atoms, as well as molecular weight of the compound),<sup>14</sup> have been successively applied to gaseous compounds. Unfortunately, such models cannot be applied to organic dusts, because they do not take into account for the granulometric distribution of the powder, which is one of the most influencing factors for the estimation of MIE.<sup>15</sup> The importance of the granulometric distribution is so relevant that several correlations for MIE determination as a function of different granulometric distribution of either the same powder or mixtures can be found in the current literature.<sup>16–18</sup>

Recently, Hosseinzadeh et al.<sup>19</sup> proposed a simple mathematical model based on the heating of a dust particle due to the energy spark in a Hartmann tube. Such a model estimates the MIE as the smallest value of energy spark at which the maximum temperature of the dust particle is equal to the ignition temperature of the particle in a dust cloud, such as that determined in a standard BAM oven, which can be considered, in some way, an experimental information equivalent to MIE.

The main aim of this work is to develop a simple mathematical model able to theoretically estimate the MIE of organic powders using very few easily accessible experimental information, such as granulometric analysis and thermogravimetric analysis (TGA). Particularly, TGA is used to determine the pyrolysis kinetics of the dust, which is then used within the model to compute the rate of combustible volatiles released by the dust particles.

## 2. METHODS AND MATERIALS

**2.1. The Hartmann Tube Test.** The MIE is usually determined using the Hartmann tube equipment, according to different standard procedures; in particular, in this work we refer to the standard procedure EN ISO/IEC 80079-20-2:2016.<sup>20</sup>

Accordingly, the electrical spark generated between the two electrodes interacts with the dust dispersed in air inside the Hartmann tube for a very short period. During this period, all the processes of heat transfer from the spark to the flammable air-dust mixture occur.

According to Sankhé et al. (2019),<sup>21</sup> the spark between the electrodes has a total duration of  $\sim 100 \mu\text{s}$ , and its extinguishing phase is characterized by an almost spherical distribution of the plasma around the electrodes. The complete extinction of the effects due to the spark lasts for  $\sim 240 \mu\text{s}$  beyond the end of the spark itself, and, at 1 ms, the phenomenon is definitively expired. During this period, the corona discharge fully develops, leading to high temperatures of the small air volume between the electrodes.

The basic idea of this work is that a spark with a given energy can ignite an air–dust mixture in the Hartmann tube test only if the discharged energy is able to heat-up the small volume of air near the electrodes above a threshold value.

Regardless how finding such a threshold value for a given dust (this will be discussed later), we must first estimate an effective value for such an air temperature, as a function of the discharged energy in the Hartmann tube test.

Temperature and size of the hot region of quasi-spherical shape (the so-called “hot core”) around the electrodes, as a function of the energy content of the spark, can be visualized during a test into the Hartmann tube using a high-frequency thermocamera, as discussed by Bu et al. (2019).<sup>22</sup> In this paper, several photographs show, for different dusts and different spark energy values, the time evolution of the quasi-spherical region around the electrodes.

In particular, from such photographs, the size of the hot core at a time equal to 0 [ms] is of interest in this work, since it can be ascribed to the spark only and not to the subsequent combustion phenomena. Actually, the pyrolysis of an organic dust cannot start before  $\sim 5$ – $10$  ms, since such a time is necessary to heat the combustible dust particles to temperature values at which the devolatilization rate is not negligible.<sup>22</sup> While the dust particles are heated, flammable volatiles from the dust pyrolysis mix with the surrounding air and they possibly start a homogeneous combustion if the mixture of flammable volatiles and air is within the flammability limits of volatiles.

Therefore, analyzing the images of the hot zone in correspondence of time equal to 0 ms, we have estimated the size of the hot core as a function of the spark energy

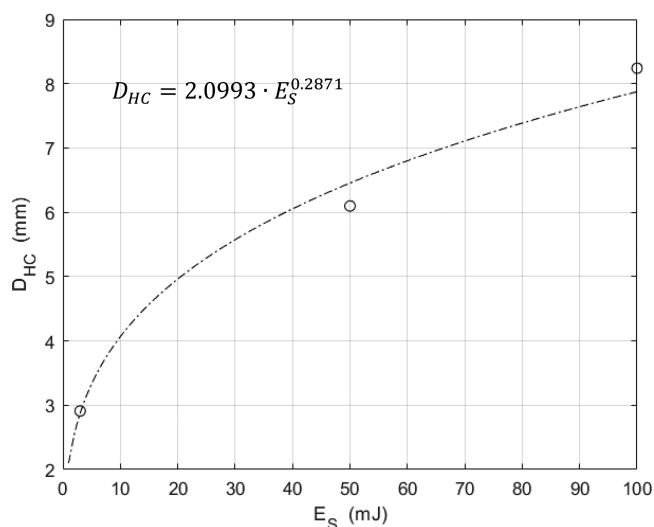


**Figure 1.** Equivalent diameter of the hot core, as a function of spark energy. Data derived from images reported in Bu et al. (2019).<sup>22</sup>

content, as summarized in Figure 1. The following relation, also reported in Figure 1, can represent these data by

$$D_{HC} = 2.0993E_S^{0.2871} \quad (1)$$

where  $E_S$  indicates the energy content of the spark [mJ], and  $D_{HC}$  represents the equivalent diameter of the hot core [mm]. Note that this relationship is obviously reliable only in the range of 3–100 mJ. Extrapolation to 1 mJ can be done with reasonable confidence, since the relationship goes to zero at the limit of  $E_S = 0$ ; otherwise, extrapolation of spark energies above 100 mJ are highly discouraged.

From this relationship, the effective temperature of the air in the hot core can be estimated (as an order of magnitude) by assuming that all the spark energy leads to an increase in the enthalpy content of such air, that is  $m \cdot C_p \cdot (T_{\text{air}} - T_{\text{amb}}) = E_S$ . Here,  $m$  is the mass of air in the hot core ( $m = \left(\frac{\pi D_{\text{HC}}^3}{6}\right) \rho_{\text{air}}$ ),  $C_p$  the specific heat at a constant pressure of air,  $T_{\text{air}}$  the effective temperature of the air in the hot core, and  $T_{\text{amb}}$  the ambient air temperature.

From such a relationship, together with eq 1, a relationship between  $T_{\text{air}}$  and  $E_S$  can be finally obtained:

$$T_{\text{air}} = T_{\text{amb}} + \frac{E_S}{\left(\frac{\pi D_{\text{HC}}^3}{6}\right) \rho_{\text{air}} C_p} \quad (2)$$

**2.2. Mathematical Model for Particle Heating and Devolatilization.** As previously mentioned, the basic idea of this work is to assume that the ignition spark creates a hot core of air able to heat up the embedded dust particles, possibly leading to their pyrolysis, and therefore to the emission of flammable volatile gases. Only when mixing such flammable volatile gases with the air in the hot core, leading to a mixture composition within the flammability range, can a homogeneous combustion start, therefore triggering the dust explosion.

While the air temperature in the hot core following a spark discharge with a given energy can be estimated as discussed in the previous section, the estimation of the volatiles–air composition requires modeling the heating, pyrolysis, and volatile emission from a particle dust surrounded by the air in the hot core. This has been done through a mathematical model derived from a literature one developed for the prediction of the deflagration index of organic dusts.<sup>11</sup> Such a comprehensive model involves a pyrolysis phase incorporating a single devolatilization step, which converts the solid to volatile compounds and a carbon residue called a “skeleton”. All the parameters needed for such a pyrolysis model can be derived from simple TGA.<sup>23</sup>

The material and energy balance equations used to model the particle heating and devolatilization are based on the following hypotheses:<sup>11</sup> one-dimensional spherically symmetric dust particle; negligible resistance to mass transfer and negligible diffusive flux, with respect to the convective one for the gas phase; no secondary reactions of the volatile pyrolysis products; local thermal equilibrium between solid and volatiles; constant heat capacity of the solid phase much larger than that of the gaseous phase; constant temperature of the air in the hot core region; pseudo-steady-state assumption for the gas phase; particles with constant volume,  $V_t$ .

**Material Balance for the Solid Phase.** Having assumed the presence of a solid residue after the pyrolysis, not all the mass of the particle leads the volatile compound; therefore, the material balance equation has been written only for the solid fraction consumed by the pyrolysis reaction ( $m_{S,r}$ ), as follows:

$$\frac{\partial m_{S,r}}{\partial t} = -r_p \cdot V_t = -k \cdot \rho_{S,r}^n \cdot V_t \quad (3)$$

Here,  $\rho_{S,r}$  is the reactive mass per unit particle volume, defined as  $\rho_{S,r} = \frac{m_{S,r}}{V_t} = \frac{m_S}{V_t} - \frac{m_{S,0} \beta}{V_t}$  and  $\beta$  is the mass fraction of the particle leading to the skeleton:  $\beta = \frac{m_{S,f}}{m_{S,0}}$ . This value can be easily derived from TGA. In this definition,  $m_{S,0}$  is the initial mass of the solid, while  $m_{S,f}$  is the skeleton mass.

By also defining the term  $\rho_{S,\text{app}}$ , which is given as  $\rho_{S,\text{app}} = \frac{m_S}{V_t} = \rho_S \cdot (1 - \varepsilon)$  where  $\varepsilon$  is the porosity of the dust particle,  $\varepsilon = \frac{V_t - V_S}{V_t} = \frac{V_v}{V_t}$  and using the relation  $\rho_{S,\text{app},0} = \frac{m_{S,0}}{V_t} = \rho_S \cdot (1 - \varepsilon_0) \approx \rho_S$ , we can derive the following expression:

$$\rho_{S,r} = \rho_{S,\text{app}} - \rho_{S,\text{app},0} \cdot \beta \quad (4)$$

Using these expressions, eq 3 leads to the following equation with the relative initial conditions:

$$\begin{cases} \frac{\partial \rho_{S,r}}{\partial t} = -k \cdot \rho_{S,r}^n \\ \text{I.C.: } \rho_{S,r}(t=0) = \rho_{S,r,0} = \rho_{S,\text{app},0} (1 - \beta) \end{cases} \quad (5)$$

This equation can be made dimensionless by defining the dimensionless particle density,  $c_S = \frac{\rho_{S,r}}{\rho_{S,r,0}} = \frac{\rho_{S,r}}{\rho_{S,\text{app},0} (1 - \beta)}$  as

$$\begin{cases} \frac{\partial c_S}{\partial t} = -k \cdot \rho_{S,r,0}^{n-1} \cdot c_S^n \\ \text{I.C.: } c_S(t=0) = 1 \end{cases} \quad (6)$$

The kinetic constant,  $k$ , can be represented by a modified Arrhenius equation, whose parameters can be also derived from TGA:<sup>23</sup>

$$k = A \exp\left[-\frac{E_a(1 - \chi\alpha)}{RT}\right] \quad (7)$$

where  $\chi$  accounts for the dependence of the activation energy on the particle conversion  $\alpha$ ,  $\alpha = \frac{m_{S,r,0} - m_{S,r}}{m_{S,r,0}} = 1 - c_S$ . This leads to the following final form of the material balance for the solid phase:

$$\begin{cases} \frac{\partial c_S}{\partial t} = -A \exp\left\{-\frac{E_a[1 - \chi(1 - c_S)]}{RT}\right\} \rho_{S,r,0}^{n-1} c_S^n \\ \text{I.C.: } c_S(t=0) = 1 \end{cases} \quad (8)$$

**Particle Material Balance for the Volatiles.** By defining the apparent volatile density,  $\rho_{V,\text{app}}$ , as  $\rho_{V,\text{app}} = \frac{m_v}{V_t} = \frac{m_v \cdot V_v}{V_t \cdot V_t} = \rho_v \cdot \varepsilon$  thanks to the pseudo-steady-state assumption, the particle material balance for the volatiles in spherical coordinates leads to the following expression:

$$\frac{\partial(v_x \rho_v \varepsilon)}{\partial r} = -\frac{2}{r} (v_x \rho_v \varepsilon) + k \rho_{S,r}^n \quad (9)$$

Introducing the new variables  $v = \rho_v \cdot \varepsilon \cdot v_x$  (which represents the massive rate of volatile gases exiting from the external surface of a single dust particle per unit particle surface) together with its ratio to  $\rho_{S,r,0}$   $V = \frac{v}{\rho_{S,r,0}}$  the final form of the material balance for the volatiles with the relative boundary condition can be obtained:

$$\begin{cases} \frac{\partial V}{\partial r} = -\frac{2}{r} V + k \rho_{S,r,0}^{n-1} c_S^n \\ \text{B.C.: } V(r=0) = 0 \end{cases} \quad (10)$$

**Particle Energy Balance.** The energy balance equation for the particle can be written as

$$\rho_{S,\text{eff}} c_{p,S} \frac{\partial T}{\partial t} = -\nabla \times (h \cdot \vec{v} + \vec{q}) - \Delta H_{\text{pyr}} k \rho_{S,r}^n \quad (11)$$

where  $\rho_{S,\text{eff}} = \rho_S(1 - \bar{\epsilon})$  is the effective particle density, using an effective average value of  $\bar{\epsilon} = 0.5$ ;  $h = \rho_{V,\text{app}} c_{p,V} T$  is the enthalpy of the volatiles per unit of volume;  $\vec{q} = -\bar{\lambda} \cdot \nabla T$  is the conductive heat flux,  $\bar{\lambda} = \lambda \cdot (1 - \bar{\epsilon})$  representing the effective thermal conductivity;  $\Delta H_{\text{pyr}}$  is the endothermic reaction enthalpy for the pyrolysis reaction. Using these definitions, the previous equation can be recast in the following one, with the relative boundary and initial conditions:

$$\left\{ \begin{array}{l} \rho_S \cdot (1 - \bar{\epsilon}) \cdot c_{p,S} \cdot \frac{\partial T}{\partial t} = \bar{\lambda} \cdot \frac{\partial^2 T}{\partial r^2} + \frac{2}{r} \cdot \bar{\lambda} \cdot \frac{\partial T}{\partial r} \\ \quad - c_{p,V} \cdot \left[ \frac{\partial}{\partial r} (v \cdot T) + \frac{2}{r} \cdot (v \cdot T) \right] - \Delta H_{\text{pyr}} k \rho_{S,r}^n \\ \text{I.C.: } T(t=0) = T_0 \\ \text{B.C.: } \left\{ \begin{array}{l} \bar{\lambda} \cdot \frac{\partial T}{\partial r} \Big|_{r=0} = 0 \\ \bar{\lambda} \cdot \frac{\partial T}{\partial r} \Big|_{r=R} = -h_c \cdot (T|_{r=R} - T_{\text{air}}) - \epsilon_{\text{em}} \cdot \sigma \cdot (T|_{r=R}^4 - T_{\text{air}}^4) \end{array} \right. \end{array} \right. \quad (12)$$

where  $h_c$  is the heat-transfer coefficient,  $\epsilon_{\text{em}}$  is the emissivity of the dust (assumed equal to 0.95), and  $\sigma$  is the Stefan–Boltzmann constant.

Note that the BCs of this equation involve the temperature of the air surrounding the dust particle, that is, the temperature of the hot core created by the ignition spark. This value can be estimated, for a given spark energy, as discussed in the previous section.

It is possible to rewrite this equation by introducing the previous dimensionless variables, as follows:

$$\left\{ \begin{array}{l} \frac{\partial T}{\partial t} = \frac{\lambda}{\rho_S \cdot c_{p,S}} \cdot \left( \frac{\partial^2 T}{\partial r^2} + \frac{2}{r} \cdot \frac{\partial T}{\partial r} \right) - \frac{(1 - \beta) \cdot c_{p,V}}{(1 - \bar{\epsilon}) \cdot c_{p,S}} \\ \quad \cdot \left[ \frac{\partial V}{\partial r} \cdot T + V \cdot \frac{\partial T}{\partial r} + \frac{2}{r} \cdot (V \cdot T) \right] - \frac{\Delta H_{\text{pyr}} \cdot (1 - \beta)}{(1 - \bar{\epsilon}) \cdot c_{p,S}} \\ \quad \cdot k \cdot \rho_{S,r,0}^{n-1} \cdot c_S^n \\ \text{I.C.: } T(t=0) = T_0 \\ \text{B.C.: } \left\{ \begin{array}{l} \frac{\lambda}{\rho_S \cdot c_{p,S}} \cdot \frac{\partial T}{\partial r} \Big|_{r=0} = 0 \\ \frac{\lambda}{\rho_S \cdot c_{p,S}} \cdot \frac{\partial T}{\partial r} \Big|_{r=R} = -\frac{h_c}{\rho_S \cdot (1 - \bar{\epsilon}) \cdot c_{p,S}} \cdot (T|_{r=R} - T_{\text{air}}) \\ \quad - \frac{\epsilon_{\text{em}} \cdot \sigma}{\rho_S \cdot (1 - \bar{\epsilon}) \cdot c_{p,S}} \cdot (T|_{r=R}^4 - T_{\text{air}}^4) \end{array} \right. \end{array} \right. \quad (13)$$

**Material Balance for the Volatiles in the Hot Core.** To know whether the concentration of the volatile gases in the hot core reaches the lower flammability limit (LFL) or not during the dust particle heating and devolatilization, the material balance equation for the volatiles in the hot core is required.

The massive rate of volatile gases leaving a single dust particle (and therefore entering the surrounding air in the hot core, possibly forming a flammable mixture) per unit area at

each moment is equal to the value of  $v$  at the outer edge of the particle, that is,  $\rho_{S,r,0} \cdot V(r=R,t)$ . Therefore, the total mass rate of volatiles entering the hot core can be computed as

$$\dot{m}_V(t) = \rho_{S,r,0} V(r=R,t) \pi D_p^2 N_p \quad (14)$$

where  $D_p$  is the particle average diameter (e.g., the  $D_{50}$  value computed from the particle size distribution of the dust);  $N_p = \frac{C_p \cdot V_{\text{HC}}}{m_p}$  (where  $C_p$  is the dust concentration in the hot core,  $V_{\text{HC}}$  is the hot core volume, and  $m_p$  is the mass of a single particle) is the number of solid particles within the hot core. The dust concentration in hot core has been estimated by assuming that the dust loaded in the Hartmann tube uniformly distribute in two-thirds of the volume of the Hartmann tube.

Therefore, the material balance equation for the volatiles in the hot core becomes

$$\frac{dm_V}{dt} = \dot{m}_V \quad (15)$$

Introducing the volatile concentration  $\rho_V$ , which is defined as  $\rho_V = \frac{m_V}{V_{\text{HC}}}$  together with eq 14, the previous equation leads to the following equation with the relative initial conditions:

$$\left\{ \begin{array}{l} \frac{d\rho_V}{dt} = \frac{\rho_{S,r,0} \cdot V(r=R,t) \pi D_p^2 N_p}{V_{\text{HC}}} \\ \text{I.C.: } \rho_V(t=0) = 0 \end{array} \right. \quad (16)$$

Equations 8, 10, 13, and 16 constitute a mixed system of ordinary and partial differential equations that, once numerically integrated, gives the space and time evolution of  $c_S(r,t)$ ,  $V(r,t)$ ,  $T(r,t)$ , and  $\rho_V(t)$ . The integration has been performed through the Method of Lines,<sup>24</sup> with the spatial derivatives approximated using a constant step, five-point centered finite difference scheme.<sup>25</sup>

In particular, during the integration of the system of equations for a given dust ignited by a spark with a given energy, the time evolution of the volatile concentration in the hot core region is computed. If such a concentration reaches (in a reasonable small time, for example, <120 ms) the lower flammability limit of the volatile gases, a homogeneous combustion can be triggered, finally leading to the dust explosion.

### 3. MIE ESTIMATION PROCEDURE

The evidence derived from the Hartmann tube experiments, together with the mathematical modeling of the dust particles heating and devolatilization, for a given dust ignited by a spark with a given energy, allow one to estimate the volatile concentration in the hot core region. If such a concentration reaches the LFL of the volatiles within 120 ms, we assume that the dust is ignited.

However, this first requires the definition of the LFL of the volatile gases produced during the dust pyrolysis. This is not a simple task, since different flammable gases can be emitted during the dust pyrolysis, possibly also changing the composition with temperature. To simplify this rough problem, it is reasonable to assume that when polymer dusts are involved, their monomers are representative of the flammability properties of the volatile gases produced, whereas, for all of the other organic dusts, methane is the species that can effectively represent the flammable properties of the



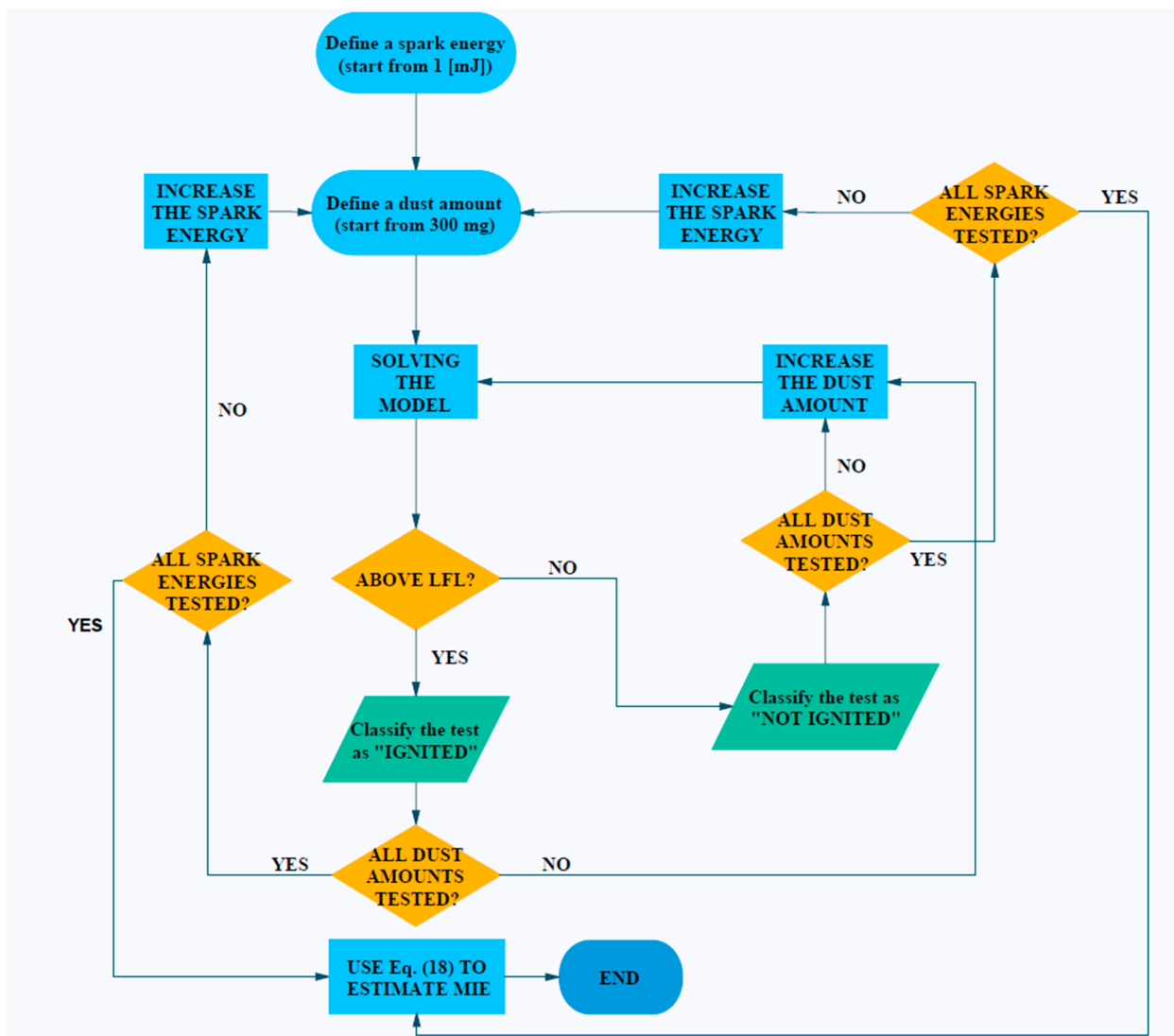


Figure 2. Flowchart of the proposed MIE estimation procedure.

volatile gases. Therefore, the LFL of the monomers (in particular, 0.9% [v/v] at 25 °C for styrene) and methane (4.95% [v/v] at 25 °C) were used in the following computations, after correcting them for the temperature influence according to eq 17.<sup>26</sup>

$$\text{LFL} = \text{LFL}_{25} - \frac{100c_{p,L}}{\Delta H_c}(T - 25) \quad (17)$$

Since this work aims to estimate the MIE values as experimentally measured in the Hartmann tube test, the experimental procedure detailed in the standard EN ISO/IEC 80079-20-2:2016<sup>20</sup> must be reproduced. In particular, this standard requires that several amounts of dust (namely, 300, 600, 900, 1200, and 1500 mg) must be loaded to the Hartmann tube and each of them must be ignited by a spark with increasing energy (namely, 1, 3, 10, 30, 100, 300, and 1000 mJ) until the dust ignition is detected. The MIE value can be then statistically calculated using the following expression:<sup>22</sup>

$$\text{MIE} = 10^{[\log_{10}(E_2) - I(E_2) \cdot (\log_{10}(E_2) - \log_{10}(E_1)) / ([NI + I](E_2) + 1)]} \quad (18)$$

where  $E_2$  is the minimum energy at which at least one of the dust amounts is ignited,  $E_1$  the maximum energy at which the ignition of all the dust amounts always fail,  $I(E_2)$  the number of dust amounts ignited at energy  $E_2$ , and  $[NI + I](E_2)$  the total number of tests (resulting in both dust ignition and dust not ignition) performed at the energy  $E_2$ .

Therefore, the procedure proposed for the estimation of the MIE of a given dust is summarized in both the following algorithm and the flowchart of Figure 2.

- (1) Define the spark energy (inside the reliability range of eq 1, therefore starting from 1 mJ).
- (2) Define the dust amount (starting from 300 mg).
- (3) Compute the hot core equivalent diameter through eq 1 and the corresponding effective air temperature through eq 2.
- (4) Integrate eqs 8, 10, 13, and 16 from 0 to 120 ms and compare the computed values of  $\rho_V$  (suitably transformed in units % (v/v)) to the corresponding LFL value at the air temperature calculated from eq 2.
- (5) If the concentration of the volatiles gases reaches the LFL value within 120 ms, the test is classified as “ignited”; otherwise, it is classified as “not ignited”.

- (6) Regardless of the test result, increase the dust amount to the following value and go back to step 3 until the last dust amount value is reached; then, increase the spark energy and repeat the procedure from step 2 onward, until the last spark energy to be verified.
- (7) Compute the MIE value using eq 18.

#### 4. RESULTS AND DISCUSSION

The proposed procedure for the estimation of the MIE was validated with comparison to the experimental results of seven different organic powders, namely, acid acetylsalicylic, cork, corn starch, niacin, polystyrene, sugar, and wheat flour.

The procedure requires the values of several parameters for each dust, such as chemical–physical parameters, kinetic parameters, and geometric parameters. While all the chemical–physical and kinetic parameters are summarized in a previous work<sup>11</sup> to which the reader is referred to, the geometric and explosibility characteristics of the considered powders are summarized in Table 1.

**Table 1.**  $D_{50}$ , Lower Flammability Limits (LFLs) at 25 °C,<sup>a</sup> and Experimental MIE Values<sup>b,c</sup>

	$D_{50}$ [ $\mu\text{m}$ ]	LFL <sub>25</sub> [% v/v]	MIE <sub>EXP</sub> [mJ]
acetylsalicylic acid	39	4.95	1
cork	17	4.95	3
corn starch	12	4.95	30
	74	4.95	88
niacin	15	4.95	1
polystyrene	40	0.90	10
sugar	34	4.95	10
wheat flour	52	4.95	30

<sup>a</sup>To be used for the LFL determination at a given temperature. <sup>b</sup>In the case of a range of MIE, the lowest value is reported. <sup>c</sup>Data values taken from refs 22 and 27–29.

The results obtained with the proposed procedure are summarized in Table 2 (in terms of E1 and E2 values, together with the corresponding I and NI values and the MIE value computed through eq 17 and in Figure 3, in terms of parity plot of experimental and estimated values.

From the parity plot of Figure 3, it is possible to notice that almost all the predicted MIE values are close or inside  $\pm 50\%$  boundaries, therefore supporting the reliability of the proposed approach.

#### 5. CONCLUSIONS

The main aim of this work was to develop a simple procedure for the estimation of the MIE of organic dusts based on accessible physicochemical properties and lumped devolatilization kinetics parameters easily obtained from simple TGA.

The procedure simulates the ignition phenomenon that occurs inside the Hartmann tube, which is the equipment most frequently used for the experimental determination of MIE, by assuming that the ignition spark suddenly heats up the air in a small volume near the electrodes, which then leads to the heating and devolatilization of the dust particles. When such a devolatilization is able to create a flammable gas mixture in the small region close to the electrodes, the dust is assumed to ignite.

The proposed procedure was validated by comparing the predicted MIE values with the experimental ones for seven

**Table 2.** Results for the Predicted MIE Values

spark energy	300 mg	600 mg	900 mg	1200 mg	1500 mg	$P = I/(I + NI)$
<b>Acid Acetylsalicylic: MIE<sub>PRED</sub> = 1</b>						
1	I	I	I	I	I	5/5
0	NI	NI	NI	NI	NI	0/5
<b>Sugar: MIE<sub>PRED</sub> = 6</b>						
10	NI	NI	I	I	I	3/5
3	NI	NI	NI	NI	NI	0/5
<b>Wheat Flour: MIE<sub>PRED</sub> = 17</b>						
30	NI	NI	I	I	I	3/5
10	NI	NI	NI	NI	NI	0/5
<b>Cork: MIE<sub>PRED</sub> = 5</b>						
10	NI	I	I	I	I	4/5
3	NI	NI	NI	NI	NI	0/5
<b>Corn Starch (<math>D_{50} = 12 \mu\text{m}</math>): MIE<sub>PRED</sub> = 13</b>						
30	I	I	I	I	I	5/5
10	NI	NI	NI	NI	NI	0/5
<b>Corn Starch (<math>D_{50} = 74 \mu\text{m}</math>): MIE<sub>PRED</sub> = 55</b>						
100	NI	NI	I	I	I	3/5
30	NI	NI	NI	NI	NI	0/5
<b>Polystyrene: MIE<sub>PRED</sub> = 55</b>						
100	NI	NI	I	I	I	3/5
30	NI	NI	NI	NI	NI	0/5
<b>Niacin: MIE<sub>PRED</sub> = 1</b>						
1	I	I	I	I	I	5/5
0	NI	NI	NI	NI	NI	0/5

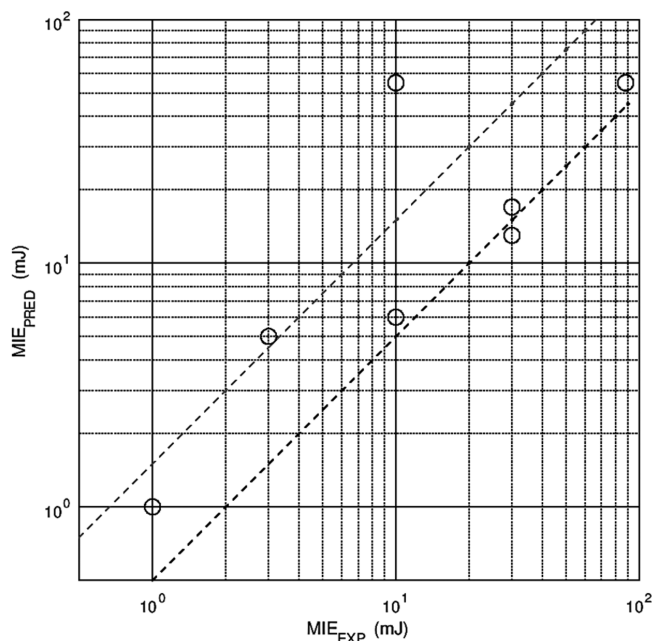


**Figure 3.** Comparison among predicted and experimental values of MIE. Dashed lines represent  $\pm 50\%$  boundaries.

organic powders: acid acetylsalicylic, cork, corn starch, niacin, polystyrene, wheat flour, and sugar. The proposed procedure allowed estimation of the values of MIE for the different organic dusts with an encouraging accuracy; indeed, the results achieved are promising and could constitute the basis for future implementation of the proposed procedure, which obviously must be further validated, independently, against a wider set of organic dusts.

Even if the experimental measure of MIE remains the safest and most accurate method for its determination, after a more complete validation, the proposed procedure could accelerate the risk analysis concerning dust explosion and, consequently, increase the safety related to both the processing and storage of potentially explosive powders.

## AUTHOR INFORMATION

### Corresponding Author

**Renato Rota** – Dip. di Chimica, Materiali e Ingegneria Chimica “G. Natta”, Politecnico di Milano, 20131 Milano, Italy; [orcid.org/0000-0002-3253-4424](https://orcid.org/0000-0002-3253-4424); Email: [renato.rota@polimi.it](mailto:renato.rota@polimi.it)

### Authors

**Sabrina Copelli** – Dipartimento di Scienza e Alta Tecnologia (DISAT), Università degli Studi dell’Insubria, 21100 Varese, Italy

**Martina S. Scotton** – Dipartimento di Scienza e Alta Tecnologia (DISAT), Università degli Studi dell’Insubria, 21100 Varese, Italy

**Marco Barozzi** – Dipartimento di Scienza e Alta Tecnologia (DISAT), Università degli Studi dell’Insubria, 21100 Varese, Italy

**Marco Derudi** – Dip. di Chimica, Materiali e Ingegneria Chimica “G. Natta”, Politecnico di Milano, 20131 Milano, Italy

Complete contact information is available at: <https://pubs.acs.org/10.1021/acs.iecr.1c00309>

### Notes

The authors declare no competing financial interest.

## REFERENCES

- (1) Increase in process safety incidents post-lockdown; available via the Internet at: <https://www.ioshmagazine.com/2020/08/04/increase-process-safety-incident-post-lockdown> (last accessed Jan. 20, 2021).
- (2) Industriall Union; available via the Internet at: <http://www.industriall-union.org/indias-safety-crisis-industrial-accidents-during-covid-19-kill-at-least-75> (last accessed Jan. 20, 2021).
- (3) Role of Operations and Maintenance in Process Safety Management. In *Guidelines for Safe Process Operations and Maintenance*; John Wiley & Sons, Ltd., 1995; pp 11–31.
- (4) Beirut Explosion: What We Know So Far. *BBC News*. Aug. 11, 2020.
- (5) Cloney, C. 2019—Dust Safety Science—Combustible Dust Incident Report, 2019.
- (6) Cloney, C. 2020—Dust Safety Science—Mid Year Combustible Dust Incident Report, 2020.
- (7) Barozzi, M.; Copelli, S.; Scotton, M. S.; Torretta, V. Application of an Enhanced Version of Recursive Operability Analysis for Combustible Dusts Risk Assessment. *Int. J. Environ. Res. Public Health* **2020**, *17* (9), 3078.
- (8) Barozzi, M.; Scotton, M. S.; Derudi, M.; Copelli, S. Recursive operability analysis as a tool for risk assessment in plants managing metal dusts. *Chem. Eng. Trans.* **2020**, *82*, 43–48.
- (9) Hassan, J.; Khan, F.; Amyotte, P.; Ferdous, R. A model to assess dust explosion occurrence probability. *J. Hazard. Mater.* **2014**, *268*, 140–149.
- (10) Fumagalli, A.; Derudi, M.; Rota, R.; Copelli, S. Estimation of the Deflagration Index  $K_{St}$  for Dust Explosions: A Review. *J. Loss Prev. Process Ind.* **2016**, *44*, 311–322.
- (11) Copelli, S.; Barozzi, M.; Scotton, M. S.; Fumagalli, A.; Derudi, M.; Rota, R. A Predictive Model for the Estimation of the Deflagration Index of Organic Dusts. *Process Saf. Environ. Prot.* **2019**, *126*, 329–338.
- (12) Scotton, M. S.; Barozzi, M.; Derudi, M.; Rota, R.; Copelli, S. Kinetic Free Mathematical Model for the Prediction of  $K_{St}$  Values for Organic Dusts with Arbitrary Particle Size Distribution. *J. Loss Prev. Process Ind.* **2020**, *67*, 104218.
- (13) Eini, S.; Jhamb, S.; Sharifzadeh, M.; Rashtchian, D.; Kontogeorgis, G. M. Developing group contribution models for the estimation of Atmospheric Lifetime and Minimum Ignition Energy. *Chem. Eng. Sci.* **2020**, *226*, 115866.
- (14) Owolabi, T. O.; Suleiman, M. A.; Adeyemo, H. B.; Akande, K. O.; Alhiyafi, J.; Olatunji, S. O. Estimation of minimum ignition energy of explosive chemicals using gravitational search algorithm based support vector regression. *J. Loss Prev. Process Ind.* **2019**, *57*, 156–163.
- (15) Castellanos, D.; Bagaria, P.; Mashuga, C. V. Effect of particle size polydispersity on dust cloud minimum ignition energy. *Powder Technol.* **2020**, *367*, 782–787.
- (16) Bisel, A.; Kubainsky, C.; Steiner, D.; Bordeaux, D.; Benabdillah, J. The minimum ignition energy of powder mixtures. *Chem. Eng. Trans.* **2016**, *48*, 433–438.
- (17) Hosseinzadeh, S.; Norman, F.; Verplaetsen, F.; Berghmans, J.; Van den Bulck, E. Minimum ignition energy of mixtures of combustible dusts. *J. Loss Prev. Process Ind.* **2015**, *36*, 92–97.
- (18) Zhang, X.; Shen, Q.; Shen, X.; Zhang, Z.; Xu, S.; Ye, S. Minimum ignition energy of medicinal powder - Florfenicol and Tilmicosin. *J. Loss Prev. Process Ind.* **2016**, *39*, 30–38.
- (19) Hosseinzadeh, S.; Berghmans, J.; Degreve, J.; Verplaetsen, F. A model for the minimum ignition energy of dust clouds. *Process Saf. Environ. Prot.* **2019**, *121*, 43–49.
- (20) Standard EN ISO/IEC 80079-20-2:2016, Explosive atmospheres—Part 20-2: Material characteristics—Combustible dusts test methods.
- (21) Sankhé, M.; Bernard, S.; Wartel, M.; Pellerin, S.; Gillard, P. Characterization of a Spark Discharge for Dust Cloud Ignition. *Contrib. Plasma Phys.* **2019**, *59* (3), 326–339.
- (22) Bu, Y.; Yuan, C.; Amyotte, P.; Li, C.; Cai, J.; Li, G. Ignition Hazard of Non-Metallic Dust Clouds Exposed to Hotspots versus Electrical Sparks. *J. Hazard. Mater.* **2019**, *365*, 895–904.
- (23) Fumagalli, A.; Derudi, M.; Rota, R.; Snoeys, J.; Copelli, S. Prediction of  $K_{St}$  Reduction with the Particle Diameter Increase for Organic Dust. *J. Loss Prev. Process Ind.* **2017**, *50*, 67–74.
- (24) Schiesser, W. *The Numerical Method of Lines*, 1st Edition; Academic Press, 1991.
- (25) Vande Wouwer, A.; Saucez, P.; Schiesser, W. E. Simulation of Distributed Parameter Systems Using a Matlab-Based Method of Lines Toolbox: Chemical Engineering Applications. *Ind. Eng. Chem. Res.* **2004**, *43* (14), 3469–3477.
- (26) Kondo, S.; Takizawa, K.; Takahashi, A.; Tokuhashi, K. On the temperature dependence of flammability limits of gases. *J. Hazard. Mater.* **2011**, *187* (1–3), 585–590.
- (27) GESTIS-DUST-EX; available via the Internet at: <https://staubex.ifa.dguv.de/?lang=e> (last accessed Jan. 18, 2021).
- (28) Addai, E. K.; Gabel, D.; Kamal, M.; Krause, U. Minimum ignition energy of hybrid mixtures of combustible dusts and gases. *Process Saf. Environ. Prot.* **2016**, *102*, 503–512.
- (29) NIOSH Pocket Guide to Chemical Hazards; available via the Internet at: <https://www.cdc.gov/niosh/npg/npgd0571.html> (last accessed March 21, 2021).